Computational Screening of HPLC-Identified Phytochemicals from Corn Silk (Stigma Maydis) as Protein tyrosine phosphatase 1B (PTP1B) Inhibitors for the Management of Type 2 Diabetes

ABSTRACT

Protein tyrosine phosphatase 1B (PTP1B) has emerged as a promising therapeutic target for the treatment of the escalating global burden of disease, diabetes, due to its critical role in insulin signaling regulation. Natural products, like those derived from a traditional plant like Corn silk, offer a valuable source of innovative antidiabetic compounds, but their bioactive constituents and molecular mechanisms remain poorly understood. This study aimed at identifying the standard constituents of Corn silk using a High-performance liquid chromatography (HPLC) approach and investigates the binding energy of potential ligands against protein tyrosine phosphatase 1B (PTP1B) target protein using a computational approach in analogy to the standard drug of diabetes. Based on molecular docking, induced-fit docking, calculation of free binding energy, and ADMET screening. 15 compounds were identified, with which most of the ligands displayed significant inhibitory activity with docking scores, ranging from -4.037 to -8.497 kcal/mol when compared with the control drug, metformin, and glyburide, with -4.624 and -0.976 kcal/mol respectively. The five top-scoring compounds showed good hydrophobic communications and hydrogen bonding associations to hinder PTP1B. The ADMET profiles of most of the compounds fell within desirable ranges, and subsequent MM-GBSA post-docking analysis validated the binding stability of selected compounds to the PTP1B protein structure. This study showed that compounds from Corn silk like

Maysin, Orientin, Quercetin, Caffeic acid, and Ferulic acid are worth further investigation as promising PTP1B inhibitors as an antidiabetic agent.

Keywords: Corn silk, PTP1B, docking studies, MM-GBSA, ADMET screening, antidiabetic

INTRODUCTION

Diabetes mellitus, a chronic metabolic disorder has been a threat to public health. It is characterized by increased glucose levels in the blood (hyperglycemia). It is also characterized by insulin resistance (lack of insulin production) or insulin sensitivity (lack of insulin to take up glucose) (Antar *et al.,* 2023). Part of the metabolic disorders associated with diabetes include impaired adipose tissue, liver, and skeletal muscle functions. Uncontrolled diabetes can lead to complications including cardiovascular disease, Kidney damage, loss of vision, coma, and in rare cases death. (Antar *et al.,* 2023; Paul *et al.,* 2023). According to WHO in 2019, 1.5 million deaths relating to diabetes were recorded, of which 48% were adults before the age of 70. The recorded death rate of disease of diabetes patients with kidney disease is 460,000 and roughly 20% of cardiovascular-related deaths are associated with diabetes. Between the years 2000-2019, the mortality rate associated with diabetes increased by 3% (WHO, 2019; Antar *et al.,* 2023). Type 2 diabetes mellitus treatment and management strategies have improved over the last few years. However, these treatment comes with financial constraints, especially in low-income countries, and serious side effects such as liver and kidney disorders, and hypoglycemia coma (Yedjou *et al.,* 2023). Hence, an urgent need for safe and effective drugs to address these complications.

A significant class of phosphatase (Protein Tyrosine Phosphatase) are signaling enzymes responsible for regulating cell activities, including cell growth, division, adhesion, and motility progression (Liu *et al.,* 2022). A member of this family is the Protein tyrosine phosphatase 1B (PTP1B) which is a major negative regulator of insulin receptor (IR) signaling that dephosphorylates IR and their binding partners for the deactivation of the pathway (Liu *et al.,* 2022; paul *et al.,* 2023). Reports of Elchebly *et al,* Showed mice with PTP1B-knockout revealed insulin sensitivity and glycemic control, they also showed resistance to obesity while having substantial triglyceride levels (Liu *et al.,* 2022; Teimouri *et al.,* 2022).

Extracts from natural plants are important sources of drugs for treating human diseases (Liu *et al.,* 2022). Recent studies revealed that anti-diabetic plants can also repair the beta-cells of islets of Langerhans (Ahmed *et al.,* 2010). The cost-effectiveness and preventive benefits of natural products make them essential in healthcare. Extracting compounds from nature could yield novel inhibitors (Jiang *et al.,* 2012). Hence, this study aims to extract the bioactive compounds isolated from corn silk (*Stigma maydis*) and predict the binding affinity against the Protein tyrosine phosphatase 1B (PTP1B) involved in diabetes mellitus. *Stigma maydis* is a dried thrum and stigma of the female flower *Zea mays* L. ssp. Mays, Poaceae (Corn plant) (Lapčík *et al.,* 2023). It is known to possess anti-diabetic, antioxidant activities, and IgE antibody inhibitors in the context of allergic diseases (Fougère *et al.,* 2023). CS extracts are employed in the treatment of urinary tract infections, malaria, and specific heart diseases. The high potassium content of CS extracts is associated with diuretic action. Moreover, research has demonstrated the anti-fatigue and anti-radiation properties of CS ethanolic extracts.

Despite all these health benefits, corn silk is often considered waste and is disposed of or burned (Lapčík *et al.,* 2023). The rising demand for organic foods has driven exponential growth in the natural antioxidant market. As a result, industries are focusing on extracting specific bioactive compounds to enhance the antioxidant potency of food products (Rahman, & Rosli, 2014). However, there is little to no study about the effect of corn silk targeting PTP1B against diabetes mellitus.

Materials and Methods

Maestro Schrodinger Suite (v12.5, 2021) was used for the computational approach of this study.

SAMPLE COLLECTION

The study utilized corn silk from corn. The corn was obtained from Shasha market, Ondo state, Nigeria, which was then taken to the Federal University of Technology, Akure, and kept at a low temperature until further analysis.

SAMPLE PREPARATION

100mg of the sample, corn silk, was weighed into a conical flask, followed by the addition of 5ml of HPLC grade Methanol (from Sigma Aldrich, Burlington, MA, USA) to dissolve the solid corn silk (Le Grand *et al*., 1988). The corn silk was filtered and the clean portion was run on HPLC.

HPLC analysis

The chromatographic analysis was performed using a Reversed-phase Agilent Technologies 1200 High-Performance Liquid Chromatography, HPLC, with the following chromatographic conditions: a Hypersil BDS C18 (Agilent) column (250mm

x 4.0 mm), and the data were analyzed using the program Class-VP version 6.10 program. The mobile phase was 0.1% formic acid + Acetonitrile (from ALPHA CHEMIKA, Mumbai India). flow rate of 0.6 mL/min; injection volume of 10 µL, and wavelength of 280 nm was used. The identification and quantification of the compounds are performed using reference standard, sodium carbonate, comparing their retention time and the UV spectrum of the peak.

LIGAND AND PROTEIN PREPARATION

The 2D structure of compounds from corn silk was retrieved from the Structure Data File (SDF) format from the PubChem database and uploaded in the workspace of Schrödinger maestro (v12.5). The LigPrep wizard of Schrödinger Maestro (v12.5) was used to convert the compounds into minimized 3D structures (Sherman *et al.,* 2006).

The 3D structure of the target protein (PDB ID: 4I8N), protein tyrosine phosphatase 1B was downloaded from the RCSB directory (https://www.rcsb.org/structure/4I8N) (Friesner *et al.,* 2004). The protein preparation wizard in Schrödinger Maestro (v12.5) was used to prepare the 3D structure of the protein for molecular docking. The structure was processed to remove any water molecules and ligands that may interfere with the docking process. The protein was also minimized to relieve any steric clashes and optimize the conformation of the binding site (Shetve *et al.,* 2020; Korkmaz *et al.,* 2022).

RECEPTOR-GRID GENERATION

The Glide module in Maestro was used to generate the Receptor grid. The grid size was defined and orientated to encompass the binding site. The grid is typically centered

around the coordinates of the co-crystallized ligand, ensuring that the docking simulations focus on the active site of the protein (Kalaycı *et al.,* 2020; Istrefi *et al.,* 2020; Akocak *et al.,* 2021). The grid box dimensions can be adjusted based on the size of the ligand and the expected binding interactions.

MOLECULAR DOCKING

Using the Schrödinger maestro (v12.5), Extra precision (XP) was chosen as the docking protocol, and the ligands were docked into the receptor grid using Glide. The scoring functions were used to predict the best ligand pose and the binding affinity was recorded (Elekofehinti *et al.,* 2020; David *et al.,* 2018).

MMGBSA Analysis

The protein-ligand complex structures resulting from the molecular docking were used for binding energy calculations, followed by the minimization of the docked complexes, carried out using Prime MMGBSA (Maffucci *et al.,* 2018; Onyeamaobi *et al.,* 2023).

ADMET analysis

Qikprop of Schrödinger maestro (v12.5) was used to predict the ADMET (absorption, distribution, metabolism, and toxicity) properties of the compounds. The physicochemical and pharmacokinetic parameters necessary for a drug to be considered as a drug candidate were determined by Lipinski's rule of five (Elekofehinti *et al.,* 2020; Yang *et al.,* 2018).

Induced-Fit Scoring (IFS)

The induced-fit docking was performed using the induced-fit docking module of Maestro v12.5. Induced fit docking was performed to account for protein flexibility and

conformational changes upon ligand binding. This allows the protein to adapt to the ligand's shape (Vijayakumar *et al.,* 2011).

RESULTS AND DISCUSSION

Table 1: Retention times of constituent peaks in HPLC-UV spectra

S/N	Identified component	Retention	Area	Height	External	Units
1.	Maysin	6.966	41.1550	3.957	4.1155	ppm
2.	Maizenic Acid	7.966	815.1310	16.979	0.0000	
3.	Caffeic Acid	9.116	64.4850	3.566	0.0000	
4.	Beta-Sitosterol	10.150	41.6010	3.971	0.0000	
5.	Daucol	10.500	73.4330	3.119	0.0000	
6.	Orientin	11.300	46.6620	2.417	0.000	

					0	
7.	Succinic Acid	11.850	41.0900	1.639	0.0000	
8.	Lycopene	12.650	48.0760	3.866	0.0000	
9.	Capsaicin	13.833	54.8770	3.748	0.0000	
10.	Quercetin	15.500	666.4750	12.864	0.0000	
11.	Kaempferol	17.233	2532.5955	35.905	0.0000	
12.	Apigenin	19.166	71.5900	5.203	0.0000	
13.	Myricetin	19.950	43.3850	3.139	0.0000	
14.	Luteolin	21.066	59.7770	5.508	0.0000	
15.	Chlorogenic Acid	3.700	1960.6550	46.581	0.0000	%
16.	P-Hydroxybenzoic Acid	5.883	527.0655	10.463	53.383	ppm
17.	Ferulic Acid	21.983	41.7330	5.909	0.0000	
18.	Vincosamide	23.083	46.4100	4.298	0.0000	

Table 2: Binding affinity of compounds extracted from corn silk against PTP1B using Maestro v12.5

Compound Name	Docking score	Compound Name	Docking score
Maysin.	-8.497	P-Hydroxybenzoic Acid.	-5.51
Caffeic Acid.	-7.548	Kaempferol.	-5.483
Ferulic Acid.	-6.923	Apigenin.	-4.937
Orientin.	-6.671	Metformin.	-4.624
Quercetin.	-6.501	Capsaicin.	-3.354
Myricetin.	-6.14	Succinic Acid.	-2.399
Chlorogenic Acid.	-6.098	Daucol.	-2.361
Luteolin.	-5.901	Beta-Sitosterol.	-2.257
Vincosamide.	-5.586	Glyburide.	-0.976

Table 3: ADMET prediction of bioactive compounds isolated from corn silk using the Qikprop module of Maestro v12.5

S/N	Compound Name	donorHB	QPlogPo/w	QPlogHERG	QPlogBB	QPlogKp	QPlogKhsa	Percent Human Oral Absorption	Rule Of Five
1.	Apigenin	2	1.605	-5.114	-1.446	-3.989	-0.039	73.192	0
2.	Beta-Sitosterol	1	7.622	-4.684	-0.354	-1.651	2.077	100	1
3.	Caffeic Acid	3	0.55	-2.191	-1.555	-4.506	-0.802	54.229	0
4.	Capsaicin	2	3.628	-4.182	-1.025	-1.849	0.19	100	0

5.	Chlorogenic Acid	6	-0.229	-3.277	-3.317	-6.191	-0.913	16.823	1
6.	Daucol	1	3.296	-2.909	0.133	-2.044	0.379	100	0
7.	Ferulic Acid	2	1.373	-2.248	-1.181	-3.683	-0.61	67.166	0
8.	Glyburide	2	4.56	-5.71	-1.994	-3.206	0.691	91.737	0
9.	Kaempferol	3	1.041	-5.201	-1.893	-4.641	-0.191	63.637	0
10.	Luteolin	3	0.926	-5.023	-1.955	-4.888	-0.198	61.205	0
11.	Lycopene	0	18.394	-7.867	2.255	1.584	3.972	100	2
12.	Maysin	7	-1.507	-5.594	-3.935	-6.882	-0.936	0	3
13.	Metformin	5	-0.69	-2.909	-1.022	-6.291	-0.915	65.566	0
14.	Myricetin	5	-0.299	-5.008	-2.948	-6.439	-0.489	26.816	1
15.	Orientin	7	-1.35	-5.293	-3.735	-7.025	-0.779	0	2
16.	P-Hydroxybenzoic Acid	2	0.581	-1.637	-0.795	-3.717	-0.802	63.978	0
17.	Quercetin	4	0.367	-5.109	-2.419	-5.544	-0.343	51.649	0
18.	Succinic Acid	2	-0.577	1.012	-1.264	-5.201	-1.192	37.179	0
19.	Vincosamide	5	0.633	-5.77	-2.068	-3.8	-0.581	66.625	0

Table 4: Free energy calculation of bioactive compounds isolated from corn silk against PTP1B using Maestro v12.5

S/N	Compound Name	MMGBSA dG Bind	MMGBSA dG Bind Hbond	MMGBSA dG Bind Lipo	MMGBSA dG Bind Solv GB	MMGBSA dG Bind vdW

1.	Maysin	-58.79	-2.85	-16.59	32.55	-50.51
2.	Caffeic Acid	-41.49	-5.44	-14.63	65.4	-24.36
3.	Ferulic Acid	-39.78	-4.98	-15.82	65.67	-25.86
4.	Orientin	-44.23	-4.87	-13.98	26.57	-26.3
5.	Quercetin	-40.87	-3.34	-13.41	24.3	-26.06
6.	Myricetin	-39.3	-3.95	-14.56	33.95	-26.43
7.	Chlorogenic Acid	-42.77	-5.68	-17.54	59.44	-31.89
8.	Luteolin	-39.65	-3.57	-11.79	31.08	-22.47
9.	Vincosamide	-40.36	-2.7	-11.56	37.09	-38.62
10.	P-Hydroxybenzoic Acid	-30.65	-4.68	-11.65	62.26	-21.24
11.	Kaempferol	-38.97	-1.94	-13.46	30.35	-24.56
12.	Apigenin	-37.55	-2.55	-11.73	23.45	-26.49
13.	Luteolin	-39.78	-3.56	-13.34	130.82	-28.76
14.	Metformin	-12.72	-2.33	-2.86	13.69	-13.49
15.	Capsaicin	-37.15	-1.27	-18.74	31.56	-33.69
16.	Succinic Acid	-14.72	-4.95	-2.01	50.26	-18
17.	Daucol	-20.25	0	-11.91	9.8	-17.24
18.	Beta-Sitosterol	-33.79	-0.14	-22.53	22.49	-35.24
19.	Glyburide	-39.06	-1.08	-15.77	34.58	-34.36

Table 5: Induced-fit docking (IFD) score of hit-compound selected from corn silk extract against PTP1B using the IFD module of Maestro v12.5

S/N	Compound Name	IFD Score
1.	Orientin.	-678.27
2.	Maysin.	-677.7
3.	Quercetin.	-675.04
4.	Caffeic Acid.	-674.81
5.	Ferulic Acid.	-673.38

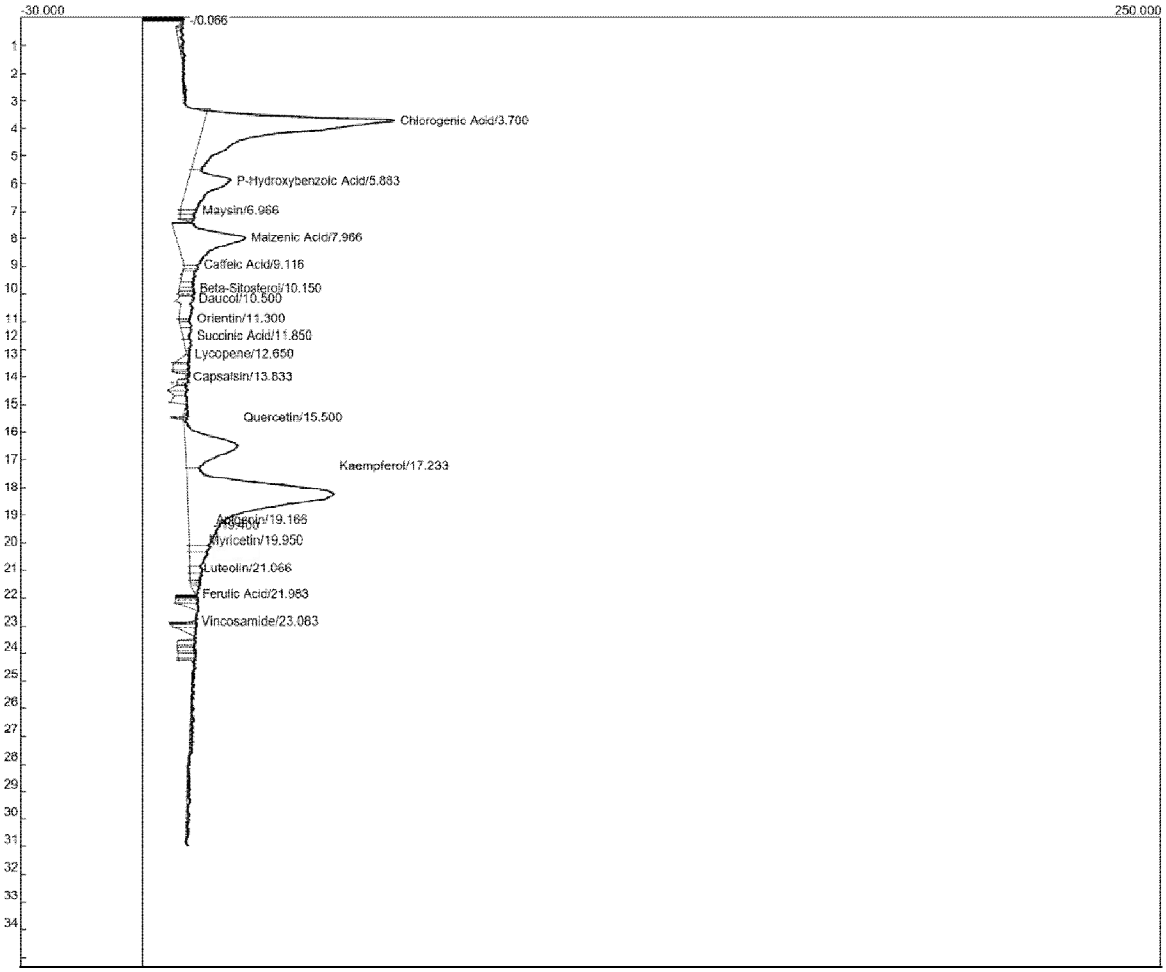

Figure 1: HPLC-UV spectra of *S. maydis* extract

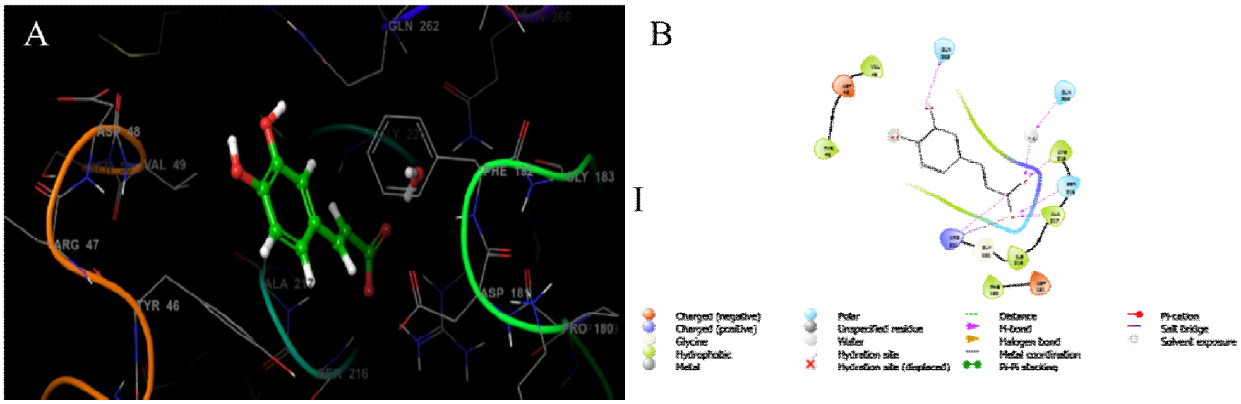

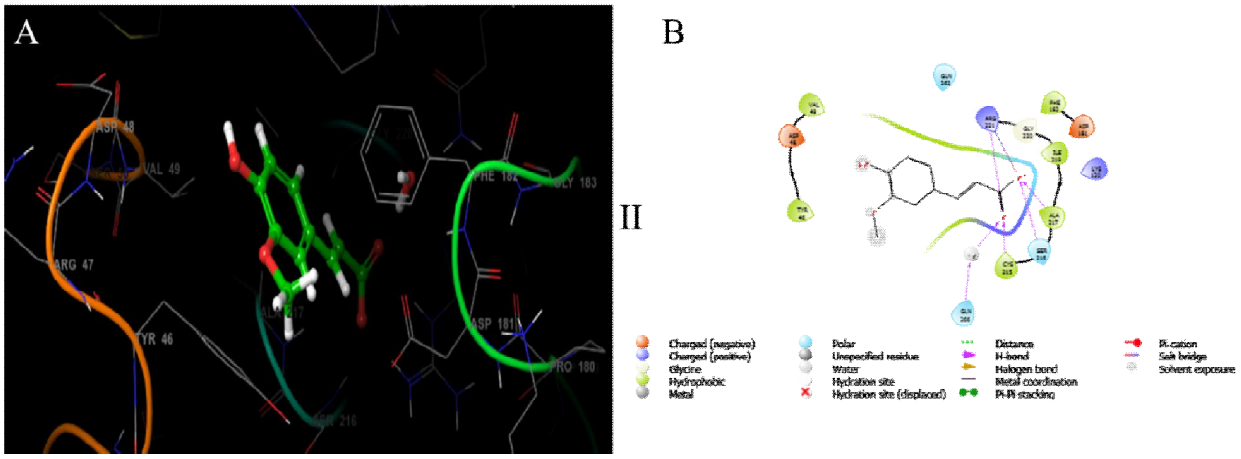
A
B
II
ASP 48
VAL 49
ARG 47
TYR 46
PHE 182
GLY 183
ASP 181
PRO 180
SER 216
Charged (negative)
Charged (positive)
Glycine
Hydrophobic
Metal
Polar
Unspecified residue
Water
Hydration site
Hydration site (displaced)
Distance
H-bond
Halogen bond
Metal coordination
Pi-Pi stacking
Pi-cation
Salt bridge
Solvent exposure

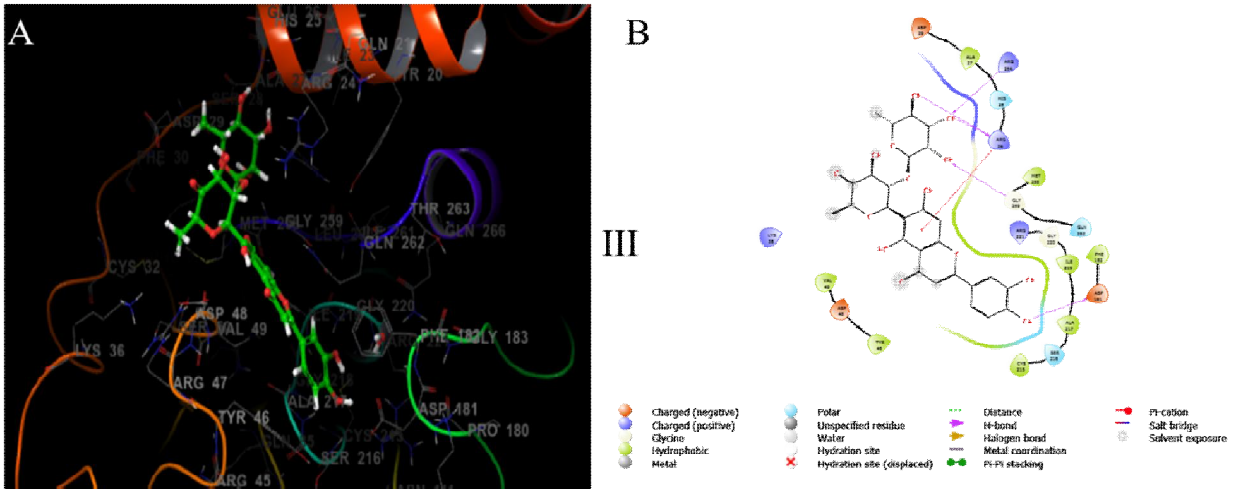
A
B
III
THR 263
GLN 262
GLY 259
CYS 32
ASP 48
VAL 49
LYS 36
ARG 47
TYR 46
PHE 182
GLY 183
ASP 181
PRO 180
SER 216
Charged (negative)
Charged (positive)
Glycine
Hydrophobic
Metal
Polar
Unspecified residue
Water
Hydration site
Hydration site (displaced)
Distance
H-bond
Halogen bond
Metal coordination
Pi-Pi stacking
Pi-cation
Salt bridge
Solvent exposure

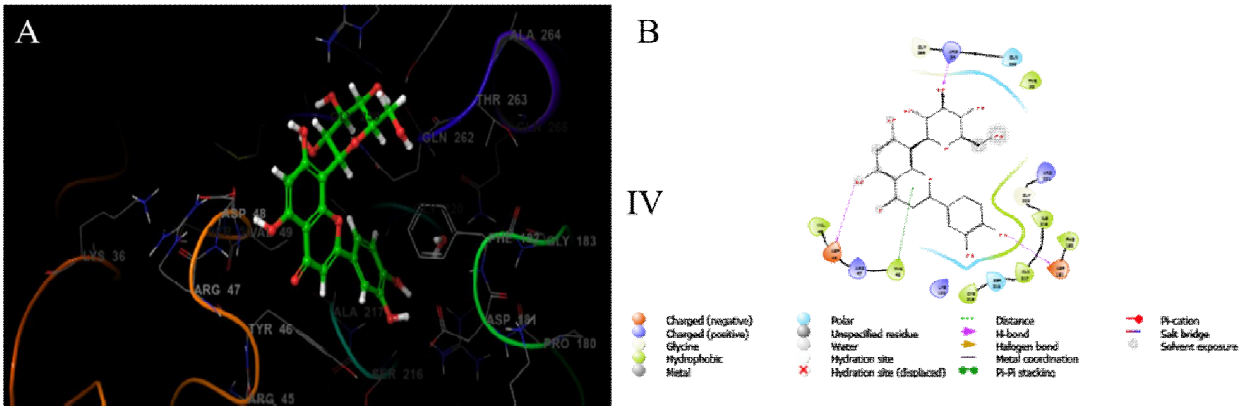
A
B
IV
ALA 264
THR 263
GLN 262
ASP 48
VAL 49
LYS 36
ARG 47
TYR 46
GLY 183
PRO 180
Charged (negative)
Charged (positive)
Glycine
Hydrophobic
Metal
Polar
Unspecified residue
Water
Hydration site
Hydration site (displaced)
Distance
H-bond
Halogen bond
Metal coordination
Pi-Pi stacking
Pi-cation
Salt bridge
Solvent exposure

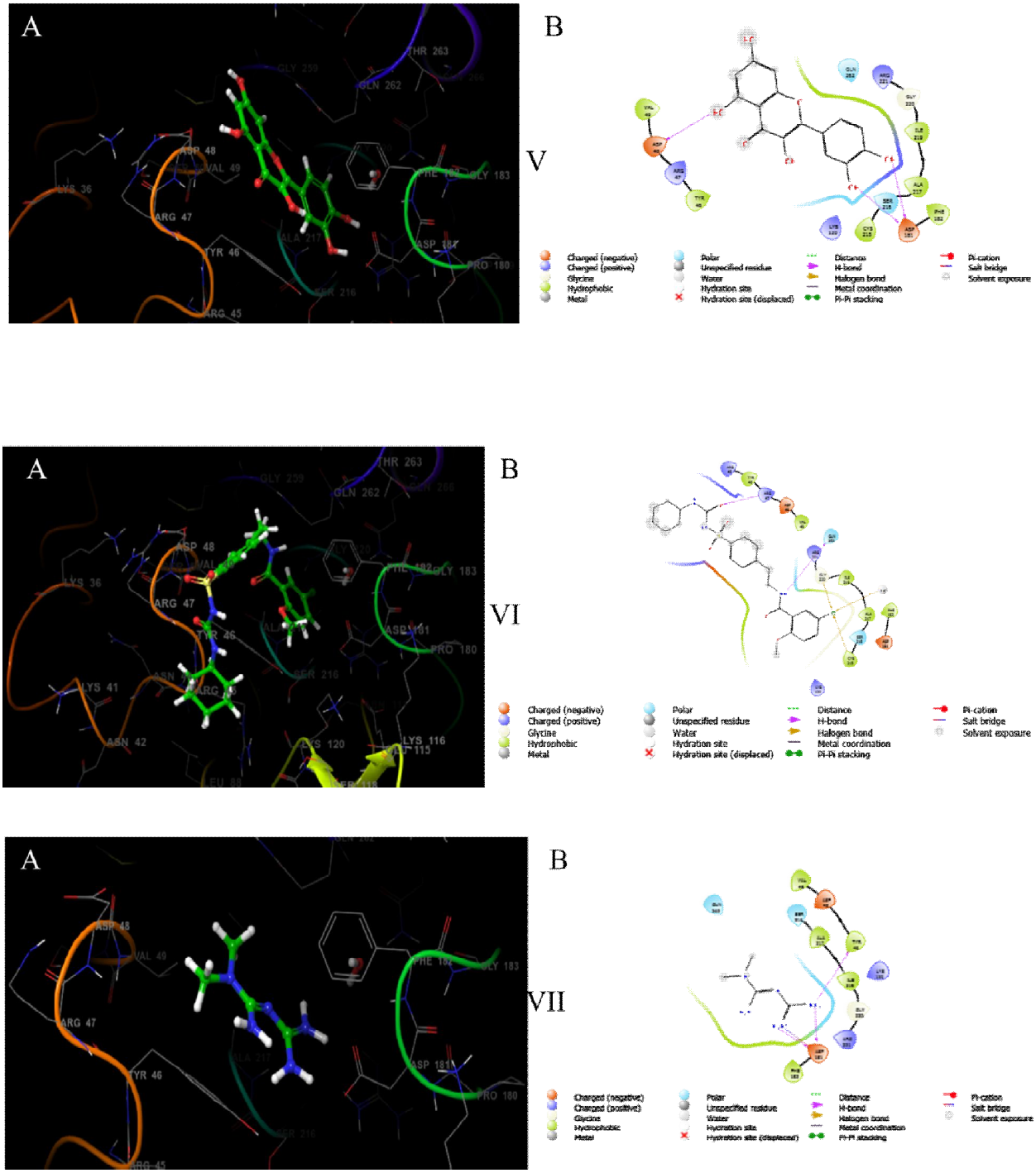

Figure 2: 2D and 3D visualization of hit-compounds in complex with PTP1B using Maestro v12.5. 2I) Caffeic acid 2II) Ferulic acid 2III) Maysin 2IV) Orientin 2V) Quercetin 2VI) Glyburide 2VII) Metformin. ‘A’ represents the 3D and ‘B’ represents the 2D of respective ligand interaction with PTP1B.

Discussion

The summary and spectrum analysis of identified compounds isolated from corn silk (*Stigma maydis*) are represented in Table 1 and Figure 1. Many classes of compounds were identified including flavonoids, alkaloids, steroids, organic acids, and terpenes. The flavonoids identified include Quercetin, Myricetin, Kaempferol, Apigenin, Maysin, Orientin and Luteolin. Caffeic acid, Ferulic acid, Chlorogenic acid, and P-Hydroxybenzoic Acid were identified as hydroxycinnamic acids. Alkaloids such as Vincosamide, and Capsaicin, Beta-sitosterol which is a steroid, Succinic acid (Organic acid), and Daucol, a sesquiterpene (a class of terpenes) were also identified. These compounds were screened and docked against PTP1B, revealing the compounds' binding energies against the protein. Metformin and Glyburide were also docked with the ligands that serve as control drugs. As seen in Table 2, Maysin revealed the highest binding affinity (-8.497 kcal/mol) to the protein followed by Caffeic acid, Ferulic acid, Orientin, and Quercetin (-7.548, -6.923, -6.671, and -6.501) kcal/mol respectively with Metformin having -4.624 kcal/mol and Glyburide having -0.976 kcal/mol. Maysin exhibits five different hydrogen bonds and pi-cation interaction. This could be the reason for its good binding affinity (Figure 2III). The hydrogen bonds were formed with enzymes via amino acids (ARG254, ARG24, GLY259, and ASP181) and pi-cation with ARG24. Ferulic acid forms hydrogen bonds with amino acids (ALA217, SER216, CYS215, GLN266, and ARG221). It also forms a salt bridge with ARG221 (Figure 2II). As well in Figure 2IV, Orientin formed three H-bonds with ASP48, ASP181, and ARG24 respectively, and formed a pi-pi stacking with amino acid residue (TYR46). Quercetin formed two H-bonds with amino acid ASP181 and one bond with ASP48. Qikprop, a

module of Maestro v12.5 is a significant tool for the prediction of absorption, distribution, metabolism, excretion, and toxicity of bioactive compounds. The number of donor HB of the compounds falls in the range of 0-7 with Maysin having the highest. The quantitative property logarithm of the partition coefficient (QPlogPo/w) is a significant parameter in assessing the compound's lipophilicity and hydrophilicity. Values between -2.0 and 6.5 are considered within a reasonable range for drug-like molecules. Higher values indicate greater lipophilicity properties and lower values indicate greater water-loving properties. All the five hit compounds were found to have higher values which display a potential advantage in the absorption, distribution, and toxicity of the compounds except for Orientin. QPlogHERG is a computational model that predicts a compound's half-maximal inhibitory concentration (IC50) value for the blockage of human ether-a-go-go-related gene (hERG) potassium channels, a key factor in cardiac repolarization. Values below -5 are considered a concern for potential hERG channel blockage. This indicates that compounds with QPlogHERG values less than -5 have a higher likelihood of causing cardiac arrhythmias. Maysin, Orientin, and Quercetin displayed good HERG values, indicating a low HERG inhibition risk. QPlogBB is a predicted parameter that estimates a compound's ability to penetrate the blood-brain barrier (BBB). A higher QPlogBB value (greater than 1.2) indicates better BBB permeability, which is crucial for drugs targeting the central nervous system (CNS). However, it's important to note that while a higher QPlogBB value is desirable for CNS drugs, excessively high values can also lead to side effects and toxicity. Therefore, a balance is needed. The results (Table 3) showed that Caffeic acid and Ferulic acid have a good range of QPlogBB values which have a good potential for CNS penetration. The compounds have % Human oral

absorption in the scope of 54-100% except for Maysin, Orientin, Chlorogenic acid, and Myricetin which displayed a relatively low percentage. Despite having good binding energy and interaction, Maysin was found to disobey 3 out of Lipinski's Rule of Five which downgraded its potential to interact with biological systems (Kalirajan *et al.,* 2019; Toppo *et al.,* 2021).

Molecular docking was complemented by MM-GBSA free energy calculations, a post-docking method that provides a more accurate estimation of binding affinities and helps to identify the most stable protein-ligand complexes. The accuracy of docking was confirmed by analyzing the lowest-energy poses. Glide score and MM-GBSA free energy calculations were performed on the docked ligand-protein complexes to evaluate the binding affinity and stability of the interactions. The result of the MMGBSA-free restricting vitality for the compounds was revealed in Table 4. The result of IDF of all the hit compounds falls between the ranges of -673.38 and -678.27 kcal/mol with Orientin displaying the highest and Ferulic showing the lowest.

CONCLUSION

The findings in this study suggest that Corn silk (Sigma maydis) generated compounds displayed higher binding affinity and interaction with PTP1B as potential inhibitor. Maysin, Orientin, quercetin, Caffeic acid, and Ferulic acid exhibited greater binding affinity than the known inhibitors of PTP1B called Metformin and Glyburide. However, this present study revealed the mentioned compounds as more suitable lead for PTP1B inhibition due to their good binding affinity, stability, and reactivity with PTP1B. This compounds could therefore serve as a lead compounds for designing inhibitors for PTP1B.

Keys: HB – Hydrogen bond; QPlogPo/w – Quality performance for predicted octanol-water partition coefficient; QPlogHERG – Quality performance for predicted IC50 value for blockage of HERG k^+ channels (Human Ether-a-go-go-Related Gene); QPlogBB – Quality performance for predicted brain/blood partition coefficient; QPlogKhsa – Quality performance for predicted binding to human serum albumin.

Disclaimer (Artificial intelligence)

Option 1:

Author(s) hereby declare that NO generative AI technologies such as Large Language Models (ChatGPT, COPILOT, etc.) and text-to-image generators have been used during the writing or editing of this manuscript.

Option 2:

Author(s) hereby declare that generative AI technologies such as Large Language Models, etc. have been used during the writing or editing of manuscripts. This explanation will include the name, version, model, and source of the generative AI technology and as well as all input prompts provided to the generative AI technology

Details of the AI usage are given below:

1.

2.

3.

REFERENCES

Akocak, S., Taslimi, P., Lolak, N., Işık, M., Durgun, M., Budak, Y. … & Beydemır, Ş. (2021). Synthesis, characterization, and inhibition study of novel substituted phenylureido sulfaguanidine derivatives as α□glycosidase and cholinesterase inhibitors. Chemistry & Biodiversity, 18(4). https://doi.org/10.1002/cbdv.202000958

Antar, S. A., Ashour, N. A., Sharaky, M., Khattab, M., Ashour, N. A., Zaid, R. T., & Al-Karmalawy, A. A. (2023). Diabetes mellitus: Classification, mediators, and complications; A gate to identify potential targets for the development of new effective treatments. *Biomedicine & Pharmacotherapy*, *168*, 115734.

David, T. I., Adelakun, N. S., Omotuyi, O. I., Metibemu, D. S., Ekun, O. E., Inyang, O. K., ... & Oribamise, E. I. (2018). Molecular docking analysis of phyto-constituents from Cannabis sativa with pfDHFR. *Bioinformation*, *14*(9), 574.

Elekofehinti, O. O. (2023). Computer-aided identification of bioactive compounds from Gongronema latifolium leaf with therapeutic potential against GSK3β, PTB1B, and SGLT2. *Informatics in Medicine Unlocked*, *38*, 101202.

Elekofehinti, O. O., Iwaloye, O., Josiah, S. S., Lawal, A. O., Akinjiyan, M. O., & Ariyo, E. O. (2021). Molecular docking studies, molecular dynamics, and ADME/tox reveal therapeutic potentials of STOCK1N-69160 against papain-like protease of SARS-CoV-2. *Molecular Diversity*, *25*, 1761-1773.

Fougère, L., Zubrzycki, S., Elfakir, C., & Destandau, E. (2023). Characterization of corn silk extract using HPLC/HRMS/MS analyses and bioinformatic data processing. *Plants*, *12*(4), 721.

Friesner, R. A., Banks, J. L., Murphy, R. B., Halgren, T. A., Klicic, J. J., Mainz, D. T., ... & Shenkin, P. S. (2004). Glide: a new approach for rapid, accurate docking and scoring. 1. Method and assessment of docking accuracy. *Journal of medicinal chemistry*, *47*(7), 1739-1749.

Ganeshpurkar, A., & Saluja, A. (2019). In silico interaction of hesperidin with some immunomodulatory targets: A docking analysis. *Indian Journal of Biochemistry and Biophysics (IJBB)*, *56*(1), 28-33.

Istrefi, Q., Türkeş, C., Arslan, M., Demir, Y., Nixha, A. R., Beydemir, Ş., & Küfrevioğlu, Ö. İ. (2020). Sulfonamides incorporating ketene N, S□acetal bioisosteres as potent carbonic anhydrase and acetylcholinesterase inhibitors. *Archiv der Pharmazie*, *353*(6), 1900383.

Kalaycı, M., Türkeş, C., Arslan, M., Demir, Y., & Beydemır, Ş. (2020). Novel benzoic acid derivatives: synthesis and biological evaluation as multitarget acetylcholinesterase and carbonic anhydrase inhibitors. Archiv Der Pharmazie, 354(3). https://doi.org/10.1002/ardp.202000282

Kalirajan, R., Pandiselvi, A., Gowramma, B., & Balachandran, P. (2019). In-silico design, ADMET screening, MM-GBSA binding free energy of some novel isoxazole substituted 9-anilinoacridines as HER2 inhibitors targeting breast

cancer. *Current Drug Research Reviews Formerly: Current Drug Abuse Reviews*, *11*(2), 118-128.

Korkmaz, I., Türkeş, C., Demir, Y., Özdemir, H., & Beydemır, Ş. (2022). Methyl benzoate derivatives: in vitro paraoxonase 1 inhibition and in silico studies. Journal of Biochemical and Molecular Toxicology, 36(10). https://doi.org/10.1002/jbt.23152

Le Grand, A., Wondergem, P. A., Verpoorte, R., & Pousset, J. L. (1988). Anti-infectious phytotherapies of the tree-savannah of Senegal (West-Africa) II. Antimicrobial activity of 33 species. *Journal of ethnopharmacology*, *22*(1), 25-31.

Liu, R., Mathieu, C., Berthelet, J., Zhang, W., Dupret, J. M., & Rodrigues Lima, F. (2022). Human protein tyrosine phosphatase 1B (PTP1B): from structure to clinical inhibitor perspectives. *International Journal of Molecular Sciences*, *23*(13), 7027.

Maffucci, I., Hu, X., Fumagalli, V., & Contini, A. (2018). An efficient implementation of the Nwat-MMGBSA method to rescore docking results in medium-throughput virtual screenings. *Frontiers in chemistry*, *6*, 43.

Onyemaobi, I. O., Jibril, S. Y., & Onyeka, P. C. COMPUTER-BASED SCREENING OF THE ANTICANCER PROPERTY OF SELECTED PANAX GINSENG PHYTO-LIGANDS.

Paul, A., Sarkar, A., Banerjee, T., Maji, A., Sarkar, S., Paul, S., Karmakar, S., Ghosh, N., & Maity, T. K. (2023). Structural and molecular insights of protein tyrosine phosphatase 1B (PTP1B) and its inhibitors as anti-diabetic agents. *Journal of*

Molecular Structure, *1293*, 136258. https://doi.org/10.1016/j.molstruc.2023.136258

Rahman, N. A., & Rosli, W. I. W. (2014). Nutritional compositions and antioxidative capacity of the silk obtained from immature and mature corn. *Journal of King Saud University-Science*, *26*(2), 119-127.

Sherman, W., Day, T., Jacobson, M. P., Friesner, R. A., & Farid, R. (2006). Novel procedure for modeling ligand/receptor induced fit effects. *Journal of medicinal chemistry*, *49*(2), 534-553.

Shetve, V. V., Bhowmick, S., Alissa, S. A., Alothman, Z. A., Wabaidur, S. M., Alasmary, F. A., ... & Islam, M. A. (2021). Identification of selective Lyn inhibitors from the chemical databases through integrated molecular modeling approaches. *SAR and QSAR in Environmental Research*, *32*(1), 1-27.

Teimouri, M., Hosseini, H., ArabSadeghabadi, Z., Babaei-Khorzoughi, R., Gorgani-Firuzjaee, S., & Meshkani, R. (2022). The role of protein tyrosine phosphatase 1B (PTP1B) in the pathogenesis of type 2 diabetes mellitus and its complications. *Journal of physiology and biochemistry*, 1-16.

Toppo, A. L., Yadav, M., Dhagat, S., Ayothiraman, S., & Eswari, J. S. (2021). Molecular docking and ADMET analysis of synthetic statins for HMG-CoA reductase inhibition activity. *Indian Journal of Biochemistry and Biophysics (IJBB)*, *58*(2), 127-134.

Vijayakumar, B., Umamaheswari, A., Puratchikody, A., & Velmurugan, D. (2011). Selection of an improved HDAC8 inhibitor through structure-based drug design. *Bioinformation*, *7*(3), 134.

WHO, Diabetes, 2019.

Yang, H., Sun, L., Wang, Z., Li, W., Liu, G., & Tang, Y. (2018). ADMETopt: a web server for ADMET optimization in drug design via scaffold hopping. *Journal of chemical information and modeling*, *58*(10), 2051-2056.

Yedjou, C. G., Grigsby, J., Mbemi, A., Nelson, D., Mildort, B., Latinwo, L., & Tchounwou, P. B. (2022). The Management of Diabetes Mellitus Using Medicinal Plants and Vitamins. *International Journal of Molecular Sciences*, *24*(10), 9085. https://doi.org/10.3390/ijms24109085

Yedjou, C. G., Grigsby, J., Mbemi, A., Nelson, D., Mildort, B., Latinwo, L., & Tchounwou, P. B. (2023). The management of diabetes mellitus using medicinal plants and vitamins. *International Journal of Molecular Sciences*, *24*(10), 9085.